Green process for chemical functionalization of nanocellulose with carboxylic acids

Etzael Espino-Perez, Sandra Domenek, Naceur Belgacem, Cécile Sillard, Julien Bras

Green Process for Chemical Functionalization of Nanocellulose with Carboxylic Acids

Etzael Espino-Pérez,[†,‡] Sandra Domenek,[‡,§] Naceur Belgacem,[†,∥] Cécile Sillard,[†] and Julien Bras*[,†,∥]

[†]University of Grenoble Alpes, LGP2, F-38000 Grenoble, France

[‡]AgroParisTech, UMR 1145 Ingénierie Procédés Aliments, 1 avenue des Olympiades, F-91300 Massy Cedex, France

[∥]CNRS, LGP2, F-38000 Grenoble, France

[§]INRA, UMR 1145 Ingénierie Procédés Aliments, 1 avenue des Olympiades, F-91300 Massy Cedex, France

Supporting Information

ABSTRACT: An environmentally friendly and simple method, named *SolReact*, has been developed for a solvent-free esterification of cellulose nanocrystals (CNC) surface by using two nontoxic carboxylic acids (CA), phenylacetic acid and hydrocinnamic acid. In this process, the carboxylic acids do not only act as grafting agent, but also as solvent media above their melting point. Key is the in situ solvent exchange by water evaporation driving the esterification reaction without drying the CNC. Atomic force microscopy and X-ray diffraction analyses showed no significant change in the CNC dimensions and crystallinity index after this green process. The presence of the grafted carboxylic was characterized by analysis of the "bulk" CNC with elemental analysis, infrared spectroscopy, and ^{13}C NMR. The ability to tune the surface properties of grafted nanocrystals (CNC-*g*-CA) was evaluated by X-ray photoelectron spectroscopy analysis. The hydrophobicity behavior of the functionalized CNC was studied through the water contact-angle measurements and vapor adsorption. The functionalization of these bionanoparticles may offer applications in composite manufacturing, where these nanoparticles have limited dispersibility in hydrophobic polymer matrices and as nanoadsorbers due to the presence of phenolic groups attached on the surface.

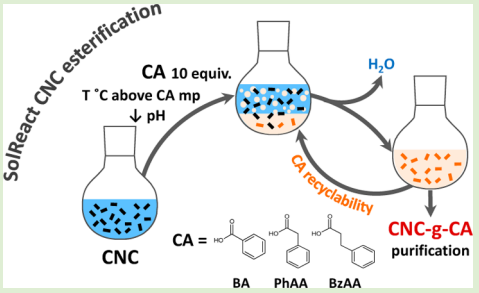

INTRODUCTION

Nanotechnology is today one of the most promising fields for developing innovative biobased materials with lowered environmental impact. Among all the possibilities, cellulose-based nanomaterials are offering important competitive advantages, not only because they come from renewable, biocompatible, sustainable, and carbon-neutral resources, but also because of their low density, high aspect ratio, high tensile strength, reactive surface, and unique optical properties.[1−5]

Among them, cellulose nanocrystals (CNC) discovered in the 60s[6−8] are generally isolated by acid hydrolysis, which degrades the amorphous regions of cellulose fibers and leaves behind the crystalline regions, that is, rod-like or whisker-shaped nanocrystals, which are less accessible to the acid degradation.[9−11]

CNC present some drawbacks and challenges, such as the difficulty to be characterized routinely, the gel-like structure at very low solid content, high price for production at large quantities, lack of standardization, agglomeration due to the strong hydrogen interaction, moisture sensitivity of CNC-based materials, and incompatibility with hydrophobic polymers for nanocomposites production.[4,12] In order to overcome these challenges, there is a worldwide research effort proved by the exponential increase of reviews, books, conferences, and patents since the 1990s.[1,13−16] Reducing the cost of these nanoparticles by developing their production at an industrial scale has been a key target in the field, and since 2011, CNC are now produced in industrial quantities in Canada, U.S.A., and Europe by several companies.[17]

The hydrophilic character of the CNC hampers their use as fillers for polymer nanocomposites with potential application in medium and high volume markets such as technical polymers or packaging. The hydrophilic surface causes compatibility problems with commonly used hydrophobic polymers. Furthermore, hydrogen bonding between CNC causes agglomeration which generates a high difficulty to redisperse the CNC powders in the nanocomposite manufacturing process.[12] However, due to the presence of a huge number of chemical functionalities (i.e., hydroxyl groups) on their structure, the nanoparticles provide a unique platform for surface modification.[18] This can be used to confer a hydrophobic behavior to the CNC surface while keeping the integrity of their crystalline core. Surface modification of CNC has already been performed to improve adhesion with hydrophobic polymers in order to enhance the reinforcement effect and at the same time limit moisture adsorption.[12] Several

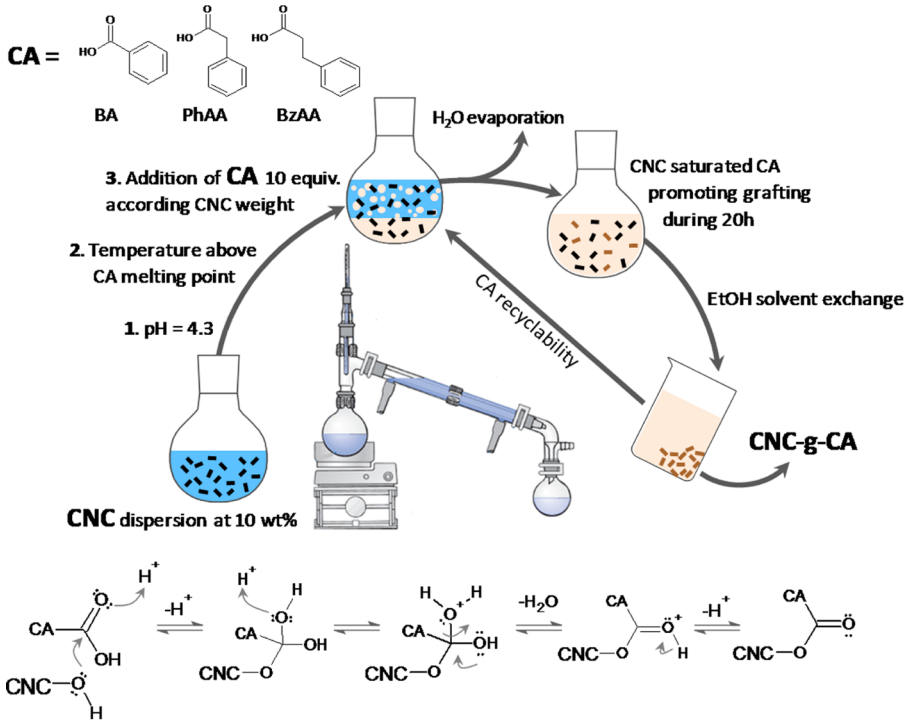

Figure 1. *SolReact* strategy and chemical mechanism for functionalization of cellulose nanocrystals with carboxylic acids.

examples of surface modification are already published in the literature and they can be classified in (i) adsorption of molecules on the CNC surface (cationic interaction),[19−21] (ii) covalent grafting of single molecules (silylation,[22] acetylation,[23−25] coupling with isocyanate derivates,[26−28] and succinic anhydride[29]), and or (iii) covalent grafting of polymer chains (by radical[30−33] and ring opening[34,35] polymerization, for example). Unfortunately, most of these techniques require the use of hazardous solvents that strongly limit the environmental benefit of the use of CNC.

Therefore, the main idea here is not only to functionalize CNC for novel applications, but also to integrate the constraints of the 12 principles of green chemistry[36] into the proposition of a grafting method. With this respect, Berlioz et al.[23] developed a solvent-free gas-phase esterification with palmitoyl chloride on freeze-dried CNC reaching a degree of substitution of 1.17 at 170 °C during 13 h. Yuan et al.[29] used an aqueous emulsion of *n*-tetradecenyl succinic anhydride and *iso*-octadecenyl succinic anhydride for grafting CNC. They absorbed the emulsion on the CNC surface and freeze-dried the system. The acetylation of CNC was then operated by an increase of the temperature to 150 °C. Both strategies need steps of drying which favor agglomeration and limit their use in some applications where redispersion is required, though. Other strategies were proposed using click chemistry[37] or creating peptide linkages between COOH and NH_2 moieties via the EDC/NHS procedure in aqueous media.[38] However, multiple reaction steps or solvent-based pretreatments to graft active moieties are needed in this case and the grafted quantity is small. Kloser et Gray[39] performed the grafting of poly(ethylene oxide) (PEO) to CNC by a "grafting-to" method. A two-step process was employed: first the CNC were desulfated with a NaOH solution, then the PEO which has been pregrafted with epoxy moiety, was grafted onto the CNC under strong basic conditions (pH ≈ 13.5) at 65 °C during 6.5 h. Espino et al.[33] used a green method for the "grafting-from" of polystyrene (PS) on CNC through aqueous free radical polymerization promoted by ozonolysis, which resulted in efficient grafting of the CNC surface.

The present paper proposes a strategy for esterification of CNC surface integrating the principles of green chemistry, such as the use of nontoxic substances, the decrease of the quantity of organic solvents and the recycling of reactants. Two main drawbacks of other published methods were thus addressed. The solvent used in the functionalization procedure equals to the reactant by an in situ solvent exchange, why the reaction can be carried out "one pot". The drying of the CNC is avoided, which minimizes the aggregation and so the redispersion issue. The proposed method is named *SolReact* because the grafted molecule plays two roles: (i) the SOLvent for avoiding drying of CNC, and (ii) the REACTive agent to be covalently attached on the CNC surface. For demonstrating the concept a structure series of aromatic carboxylic acids was used, where the specific molecules were selected among substances usually used for flavouring, food additives, fragrance, fixative and preservative agent. The esterification of the CNC was monitored with infrared spectroscopy and ^{13}C NMR. The surface grafting efficiency was evaluated with X-ray photoelectron spectroscopy, and the impact of grafting on the surface properties of the CNC was analyzed.

EXPERIMENTAL SECTION

Materials. Microcrystalline cellulose (MCC) powder acquired from Sigma-Aldrich (France) was used as raw material for the production of cellulose nanocrystals (CNC). Sulfuric acid (>95 wt %) and ethanol were purchased from Chimie-Plus (France). Benzoic acid (BA) at 99% (p.a. quality), phenylacetic acid (PhAA) at 99% (p.a. quality), and benzylacetic acid (hydrocinnamic acid, 3-phenylpropanoic acid; BzAA) at 99% (p.a. quality) were acquired from

Aldrich (France). Sodium chlorite, sodium hydroxide, and sodium chloride were purchased from Roth (France).

Production of Cellulose Nanocrystals. The preparation of CNC followed an adaptation of the optimized protocol of Bondeson et al.[9] MCC at 7.1 wt % was dispersed in water. Sulfuric acid was added slowly to a concentration of 64 wt %. The CNC in the acid suspension was then hydrolyzed at 44 °C for 130 min under mechanical stirring. The excess of sulfuric acid was removed by cycles of water exchange/centrifugations. After, the resulting suspensions containing the nanocrystals were dialyzed in deionized water during 1 week until neutral pH, and homogenized using an Ultra-Turax T25 homogenizer (France). Finally, samples were subjected to ultrasound probe (Branson 250 Sonifier) during 5 min at 40% of amplitude in order to ensure good dispersion of the nanocrystals, neutralized, and stored at 4 °C. A drop of chloroform was added in order to avoid microbial development.

Chemical Modification of Cellulose Nanocrystals. A scheme of the *SolReact* method is given in Figure 1. A closed distillation system was used for water evaporation. It was equipped with a condenser held at 5 °C. The aqueous CNC suspension at 10 wt % was fabricated by ultrasound treatment for 3 min. The pH was adjusted to 4.3 with HCl (0.1 mol·L^{-1}). The balloon flask with the CNC dispersion was mounted to the distillation system and placed in an oil bath at 130 °C. After 10 min, an excess of carboxylic acid (CA; 10 equiv according to the CNC dry weight) were added slowly in order to ensure the melting of the CA and its adsorption on the CNC surface. The system was kept under agitation during 20 h at the 130 °C, a temperature higher than the melting point of the specific CA reactant for performing the CNC surface esterification.

After the reaction, the product CNC-*g*-CA was purified from unreacted CA by 6 times dispersion-centrifugation with a large excess of ethanol at room temperature. Ethanol is a good solvent for the different carboxylic acids used (10000 rpm at 4 °C for 10 min). The dispersion-centrifugation washing is a purification method adapted to nanoscale objects and comparable in efficiency to Soxhlet extraction as previously shown.[27] Therefore, the characterized CNC-*g*-CA corresponds to the grafted carboxylic acid on CNC.

The carboxylic acids dissolved in the washing ethanol were recycled by distillation of the solvent in a rotavapor during 3 h.

Characterization of Cellulose Nanocrystals. *Atomic Force Microscopy (AFM).* Atomic force microscopy was used to ascertain and compare the crystal morphology of different CNC obtained. Measurements were performed on a Multimodal AFM (DI, Veeco, Instrumentation Group) in tapping mode. CNC were observed after spin-coating of CNC suspension at 0.01 wt % on a mica substrate and dried at room temperature.

X-ray Diffraction (XRD). X-ray analyses were performed using a Panalytical X'Pert Pro MPD-Ray diffractometer equipped with an X'celerator detector and operated with Ni-filtered Cu, Kα radiation (λ = 1.54 Å) generated at a voltage of 45 kV and current of 40 mA. Scans were performed from 5° to 60°. The CNC crystallinity index was evaluated using the Buschle-Diller and Zeronian equation:

$$I_c = 1 - \frac{I_1}{I_2} \tag{1}$$

where I_1 is the intensity at the minimum (2θ = 18.8°) and I_2 is the intensity associated with the crystalline region of cellulose (2θ = 22.7°). All analyses were at least duplicated.

Infrared Spectroscopy (IR). IR spectra of modified and unmodified CNC were performed in the form of KBr pellets by transmission on a PerkinElmer, Spectrum 65. All spectra were recorded in the frequency range of 4000−500 cm^{-1}, with a resolution of 4 cm^{-1} and 16 scans. Spectra were recorded at least twice with different samples to check reproducibility and the most representative spectra were shown for discussion.

Elemental Analysis. Elemental analysis was carried out by the "Service Central d'Analyse (Vernaison, France)" of the "Centre National de la Recherche Scientifique (CNRS)". Carbon, hydrogen, and oxygen contents were measured for unmodified and modified CNC. The precision of the measurement is usually higher than the standard deviation and is commonly taken to be ±0.2 wt % at maximum. The collected data allowed determining the degree of substitution (DS), which corresponds to the number of grafted hydroxyl groups per anhydroglucose unit (AGU) according to the following equation:

$$DS = \frac{C_{AGU} - X_c \cdot AGU}{X_c \cdot CA - C_{CA}} \tag{2}$$

where X_c is the measured weight fraction of carbon in the sample, C_{AGU} is the carbon mass (72 g·mol^{-1}/AGU), and AGU the total mass of an anhydroglucose unit (162 g·mol^{-1}), C_{CA} the carbon mass of the carboxylic acid (96 g·mol^{-1}/PhAA, 108 g·mol^{-1}/BzAA) and CA is the total mass of the carboxylic acid (137 g·mol^{-1}/PhAA, 150 g·mol^{-1}/BzAA). The analyses were performed twice and the average was used.

Solid-State Nuclear Magnetic Resonance (NMR). Solid state ^{13}C NMR experiments were performed on Bruker AVANCE 400 spectrometer. All spectra were recorded using a combination of cross-polarization, high power proton decoupling, and magic angle spinning (CP/MAS). ^{13}C spectra were acquired at 298 K, with a 4 mm probe operating at 100.13 MHz. MAS rotation was 12 kHz, CP contact times 2 ms and repetition time 1 s. The chemical shift values were measured with respect to TMS via glycine as a secondary reference with the carbonyl signal set to 176.03 ppm.

X-ray Photoelectron Spectroscopy (XPS). XPS experiments were carried out using a PHI Quantera SXM instrument (Physical Electronics, Chanhassen, U.S.A.) equipped with a 180° hemispherical electron energy analyzer and a monochromatized Al Kα (1486.6 eV) source operated at 15 kV under a current of 4 mA. The analyses were done with a depth lower than 5 nm (around 3 nm). The analysis spot had a diameter of 200 μm and the detection angle relative to the substrate surface was 45°. Insulating samples were analyzed with dual-beam charge neutralization and the C−C/C−H component of the C 1s peak was adjusted to 285 eV.

Contact Angle Measurements. The dynamic behavior of the contact angle for a drop of deionized water (purified by micropore) on the surface of a film of unmodified CNC and pressed pastilles of modified CNC was measured during 1 min before the water absorption by the sample. The measured contact angle was used in Young's equation:[40]

$$\gamma_{lv} \cos \theta_\gamma = \gamma_{sv} - \gamma_{sl} \tag{3}$$

where γ_{lv}, γ_{sv}, and γ_{sl} are the surface tensions of the liquid−vapor, solid−vapor, and solid−liquid interfaces, respectively, and θ_γ is the contact angle. The work (W_{sl}) required to separate a unit area of the solid−liquid interface, related to the work of adhesion per unit area of a solid and liquid, is obtained using eq 4:

$$W_{sl} = \gamma_{lv} + \gamma_{sv} - \gamma_{sl} \tag{4}$$

Equations 2 and 3 together give W_{sl} as a function of only γ_{lv} and θ_γ:

$$W_{sl} = \gamma_{lv}(1 + \cos \theta_\gamma) \tag{5}$$

A DataPhysics contact angle instrument equipped with a CCD camera was used, allowing the determination of the contact angle at equilibrium with a precision of ±1°. The kinetics of its evolution was followed a few tens of milliseconds after the deposition of the drop by taking up to 1000 images per second. Each reported value of W_{sl} is the average of at least triplicate measurements.

Dynamic Vapor Sorption. Dynamic vapor sorption (DVS) was used to assess the moisture adsorption of CNC before and after modification on sample powders dried from acetone and previously conditioned at 0% relative humidity (RH) over P_2O_5 during at least 3 weeks. Sorption profiles were determined using a Surface Measurement Systems (London, U.K.) Intrinsic DVS apparatus. Approximately 10 mg of powder samples were analyzed. The studied relative humidities were 0, 40, and 80%. Equilibrium sorption at each RH was determined by a change in mass to time ratio of 0.002 dm/dt. Each characterization was at least done in duplicate.

Thermogravimetric Analysis (TGA). TGA was carried out by employing a thermogravimetric analyzer PerkinElmer, STA 6000.

Samples were heated from 30 to 800 °C under a stream of nitrogen of 100 mL·min^{-1} at a heating rate of 10 °C·min^{-1}.

RESULTS AND DISCUSSION

Morphological and Structure Characterization of Neat and Functionalized CNC. CNC were prepared by sulfuric acid hydrolysis of microcrystalline cellulose. A gel-like suspension at 2.4 wt % of CNC was achieved. At low concentration (around 0.5 wt %), the CNC suspension showed strong shear birefringence when observed by cross-polarized light (Figure 2a) due to the polarization of plane light by nematic orientation of the nanocrystals.[41,42]

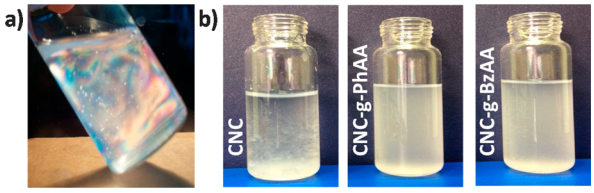

Figure 2. (a) Birefringence behavior of cellulose nanocrystals, and (b) neat and grafted cellulose nanocrystals dispersed in chloroform (0.5 wt %).

The results of the morphological analysis of the nanocrystals are given in Figure 3, which plots the histograms of length and width of CNC obtained by AFM analysis coupled to *ImageJ* image treatment. CNC keep their rod-like shape even after chemical grafting. Slight, but not statistically significant reduction of length (L) and width (d) can be observed after the chemical functionalization, principally in the case of PhAA. Considering the standard deviation (detailed in Figure 2), the acidic treatment did not change the CNC length but slightly the width. This can probably be attributed to a peeling effect from the surface of highly grafted cellulose as already observed by others[43] or to degradation of the native cellulose because of the acidic conditions used for the reaction (like in vegetable parchment cellulose sulfurization).[44] The compatibility of the neat cellulose nanocrystals with hydrophobic systems is low because of the hydrophilic nature of the CNC surface. Figure 2b shows the improving CNC dispersion in an organic solvent after surface grafting. The modified CNC were homogeneously distributed in chloroform, while neat CNC aggregated and sunk to the ground.

The change of the crystalline structure of CNC was checked by the analysis of the X-ray diffractograms for all CNC samples (Figure 4). All samples have a crystalline organization as shown by the presence of the signal 110 (15.8°), 200 (22.7°), and 004, which are characteristics of the cellulose I crystalline form. From this information, the crystallinity index (χ_c) of the unmodified and modified was calculated by the peak height method.[45,46] The values of χ_c were 84, 77, and 76% for CNC, CNC-*g*-PhAA, and CNC-*g*-BzAA, respectively. Functionalization did, therefore, not create cellulose II, a result also observed using other grafting methods.[45] Only a slight decrease (less than 10%) of χ_c was measured after the chemical functionalization. This slight loss of crystallinity is most probably related to acid conditions and high temperatures used to promote the esterification reaction, as already discussed in previous works on the hydrolysis conditions for CNC obtention.[47−49]

***SolReact* Chemical Modification of Cellulose Nanocrystals.** The *SolReact* method (scheme in Figure 1) was used

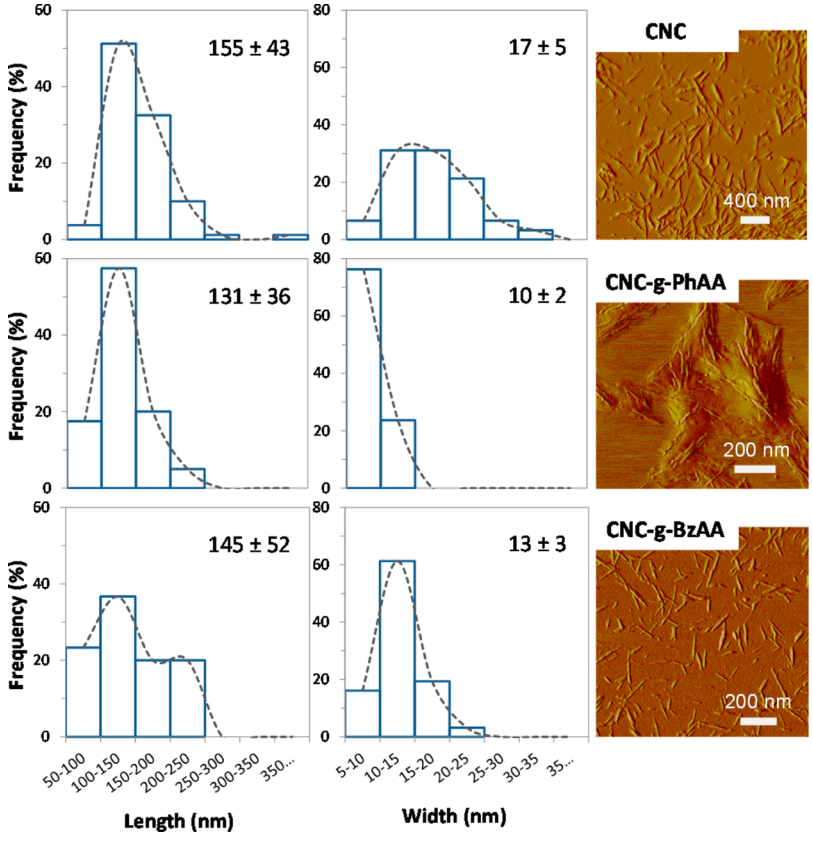

Figure 3. Histograms of CNC dimensions obtained by analysis by AFM/*ImageJ*, and AFM micrographs of neat and modified CNC.

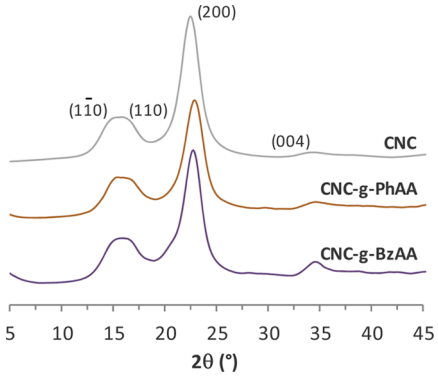

Figure 4. X-ray diffractograms of neat CNC and CNC modified with PhAA and BzAA.

for the esterification of CNC by aromatic carboxylic acids (CA). The procedure responds to the following criteria of green chemistry: the use of an aqueous suspension and nontoxic carboxylic acids for grafting, relatively low reaction temperature, reaction at ambient pressure, and the possibility of recycling of excess reactant by solvent distillation.

To our knowledge, this is the first time such a strategy is proposed for CNC surface chemical modification.

The key innovation of the *SolReact* process is the addition of the CA at a temperature over its melting point and at a temperature higher than the boiling point of water. This allows for efficient esterification due to water distillation following Le Chatellier's principle and the saturation of CNC with the melted carboxylic acid at low pH. At the same time the distillation provokes an in situ solvent exchange from water to the reactant without drying of CNC.

The reaction mechanism is presented in Figure 1. The CA presents a delocalization due to the acid conditions. An electron pair from the hydroxyl group of the CNC reacts with the carbocation of the CA. Due to the instability of the complex, water is lost and goes into the reaction solvent upon stabilization of the CNC ester. Usually a catalyst is used. In our case, residual sulfate groups at the surface of CNC might play this role.

The optimized reaction parameters were a pH of 4.3, which is roughly equal to the pK_a of the used carboxylic acids and a temperature of 130 °C, which is above the water boiling point and CA melting, below CA evaporation, and still moderate for avoiding CNC degradation. (For a description of the physical, chemical, and safety features of the molecules used in this study, see the Supporting Information, Table S1.)

The chemical grafting of CNC was followed by FT-IR spectra of neat and functionalized CNC detailed in Figure 5. It is worth noting that all grafted CNC were washed to eliminate all residual reactants before analysis (as detailed in experimental part). After the chemical modification in the case of PhAA and BzAA, a new band was observed around 1730 cm^{-1} which corresponds to the C═O vibrations from the ester functions of the carboxylic acids. In the case of BA, no carboxylic band was observed. No bands at 1700 cm^{-1} related to carboxylic acid reagent were observed for functionalized samples proving the efficiency of the washing step. Peaks between 3100 and 3000 cm^{-1} are assigned to aromatic C−H vibrations, around 1520 cm^{-1}, bands are associated with C−C vibrations in the aromatic ring. At 2922 and 2855 cm^{-1} there are the bands that correspond to aliphatic C−H stretches. This first characterization evidence grafting of cellulose in the case of PhAA and

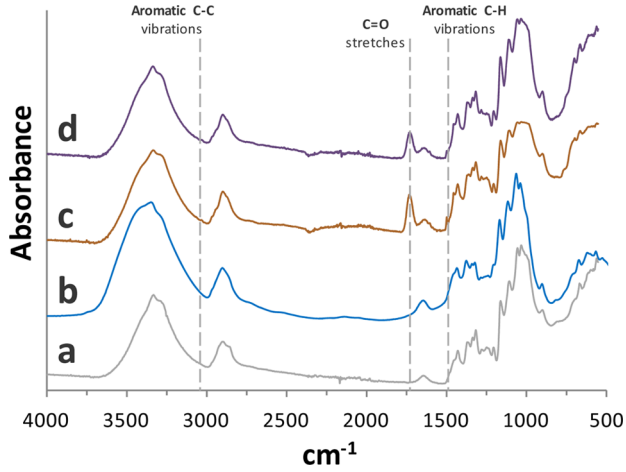

Figure 5. FT-IR spectrum of (a) neat CNC and functionalized CNC with (b) BA, (c) PhAA, and (d) BzAA.

BzAA. In the case of BA, FT-IR bands linked to grafting were absent of the spectra. The reason for unsuccessful reaction was caused by the delocalization of the carboxyl double bond with the neighboring aromatic ring which prevents or limits BA reactivity. Moreover, its higher melting temperature might favor aggregation of CNC.

The unsuccessful reaction with BA showed the importance of proper carboxylic acid selection for the application of the *SolReact* method. In conclusion, carboxylic acids need to hold the following features in order to be successfully grafted on the CNC surface:

(i) Inert toward water, but miscible.
(ii) Melting point below water evaporation and boiling point higher than 150 °C.
(iii) Low acid behavior and no cellulose swelling to limit CNC structure deterioration or bulk grafting.
(iv) Reactive (nondelocalized) at sufficiently high pH.

Bulk Characterization of the Grafting Efficiency. For evaluating the functionalization efficiency of PhAA and BzAA, elemental analysis was used and the degree of substitution (DS) determined (Table S2 in the Supporting Information). Theoretically, the weight ratio between oxygen and carbon atoms of the anhydroglucose unit is 1.11, which corresponds to an elemental weight fraction of 44.4 and 49.4% of carbon and oxygen, respectively. However, the experimental weight ratio (O/C) of neat CNC here is 1.23. It is well-known that this difference can be explained by the presence of some oxygen-rich impurities, the presence of sulfate groups on the cellulose chain and by experimental error. A correlation has already been proposed[27] to correct the differences between theoretical and experimental results (The corrected values are displayed in table S2, in Supporting Information). A clear increase in the carbon content is obtained for grafted CNC and the ratio O/C changed from 1.11 (corrected values) to 0.83 for CNC-*g*-PhAA and 0.91 for CNC-*g*-BzAA. This is in accordance with our expectation that the carbon percent increases from CNC to BzAA then PhAA. The DS values were obtained from the corrected values according to eq 2 from the weight fraction of carbon showing successful grafting of 50 and 30 molecules of carboxylic acid per 100 AGU. The drawback of the elementary analysis method is however that the results are an average over the totality of the bulk CNC.

In order to further evidence grafting on CNC, solid state ^{13}C NMR was also performed and spectra are shown in Figure 6.

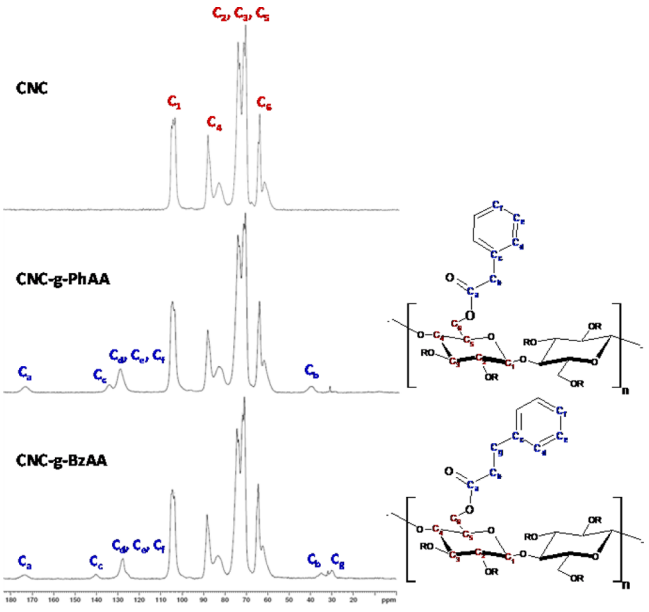

Figure 6. ^{13}C solid state NMR spectra of neat and carboxylic acid grafted CNC.

The region of the carbons signals due to the AGU extends from 60 to 106 ppm. C_4 and C_6 show a split into a contribution of the amorphous nonhydrolyzed cellulose chains (at high frequencies), which are located on the surface, and the signal from the crystalline part (at low frequencies). C_2, C_3, and C_5 are found between 70 and 75 ppm and these atoms do not participate in the $\beta(1-4)$ linkage. Because of the electronegativity differences in the C_1 environment, its signal is placed at lower frequencies (105 ppm). Upon grafting, new signals appeared: four and five characteristic resonance peaks were detected after the grafting of PhAA and BzAA, respectively. At high frequencies carbons from methylene group are detected, C_b for PhAA (40 ppm), and C_b and C_g for BzAA (35 and 32 ppm). A difference is observed when both C_b are compared; the C_b PhAA is placed at lower frequencies because of its direct linkage with the carbonyl and phenyl group. The region between 126 and 128 ppm is assigned to all protonated aromatic carbons (C_d, C_e, and C_f), while the peaks at 134 and 140 ppm are related to the nonprotonated aromatic carbon (C_c). Finally, carbon from the carbonyl group (C_a) was detected at the highest frequency (173 ppm).

Surface Characterization of the Grafting Efficiency. The main target of the *SolReact* method is efficient surface modification with keeping intact the crystalline CNC core. Therefore, X-ray photoelectron spectroscopy was performed to investigate the CNC surface nature. Indeed, XPS has already proved excellent performance in the characterization of cellulose surface modification and it has been used since around 20 years by Belgacem's group.[50] The full XPS spectra recorded for neat and modified CNC are shown in Figure 7. A quantitative XPS analysis can be done by calculating the atomic concentrations from the peak areas of the photoelectron using Gaussian−Lorentzian deconvolution. Pure cellulose exhibits two principal peaks around 532 and 285 eV in the full spectra, which correspond to the oxygen and carbon, respectively. Furthermore, a small sulfur peak at 168 eV due to surface

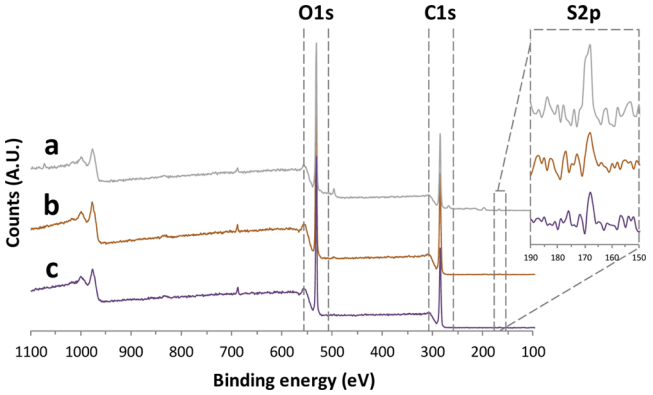

Figure 7. Wide scan XPS spectra of (a) unmodified CNC and modified CNC with (b) PhAA and (c) BzAA.

sulfation caused by the acidic MCC hydrolysis for CNC production can be detected.[51]

These XPS results clearly evidence the occurrence of an ester group due to covalent bonding between the carboxylic acid molecules and the hydroxyls on the CNC surface. (The surface functional group composition and the ratios of oxygen-to-carbon (O/C) are presented in Table S3 in Supporting Information). The neat CNC showed a molar O/C ratio of 0.82 close to that one of pure cellulose (0.83).[50,52] The carbon percentage values of neat CNC were higher than expected. This difference can be attributed to some fatty acid impurities. As expected, the O/C ratio for all modified CNC decreased in comparison to neat CNC. The percent of carbon after the functionalization with PhAA and BzAA was in good agreement with the results from elemental analysis, considering that XPS analysis takes place approximately at 3 nm from the surface and is therefore more sensitive to impurities.

One big advantage of the XPS analysis is the information that can be obtained about the degree of substitution in the surface (DSS) by the deconvolution of the C 1s signal shown in Figure 8. When regarding the deconvoluted curves, pure cellulose exhibits two peaks related to C−O (alcohols and ethers) and O−C−O (acetal) moieties.[50] In practice (Figure 8b, and Table S3 in Supporting Information), the XPS analysis of nanocellulose reveals usually four C1 peaks at 285.0, 286.3, 287.7, and 288.9 eV related to C1 (C−C/C−H), C2 (C−O), C3 (O−C−O/C═O), and C4 (O−C═O), respectively:[35]

(a) C1 peak at 285.0 eV is not present in pure cellulose, and this signal is the contribution of the presence of nonoxidized alkane-type carbon atoms and impurities like lignin, extractives, and fatty acids.[50]

(b) C2 peak at 286.3 eV corresponds to the presence of ether groups (C_5-O-C_1 and C_1-O-C_{4*}), the unmodified C−OH of the glucose ring, and the hydroxyl end of the cellulose chains. This peak is the contribution of all six carbon atoms (C_1-C_6) in Figure 8a.

(c) C3 peak at 287.7 eV is attributed to acetal moieties and this signal is the contribution of the C_1 of the AGU unit. Here, this signal is not expected to change much after the chemical modification since there are no hydroxyl groups attached to this carbon atom, except for the low quantity of hydroxyl end groups of the cellulose chain, and a possible steric effect of the carboxylic acids during the XPS analysis.

(d) C4 peak at 288.9 eV is the contribution of esters groups, which is absent in pure cellulose samples. Its presence in

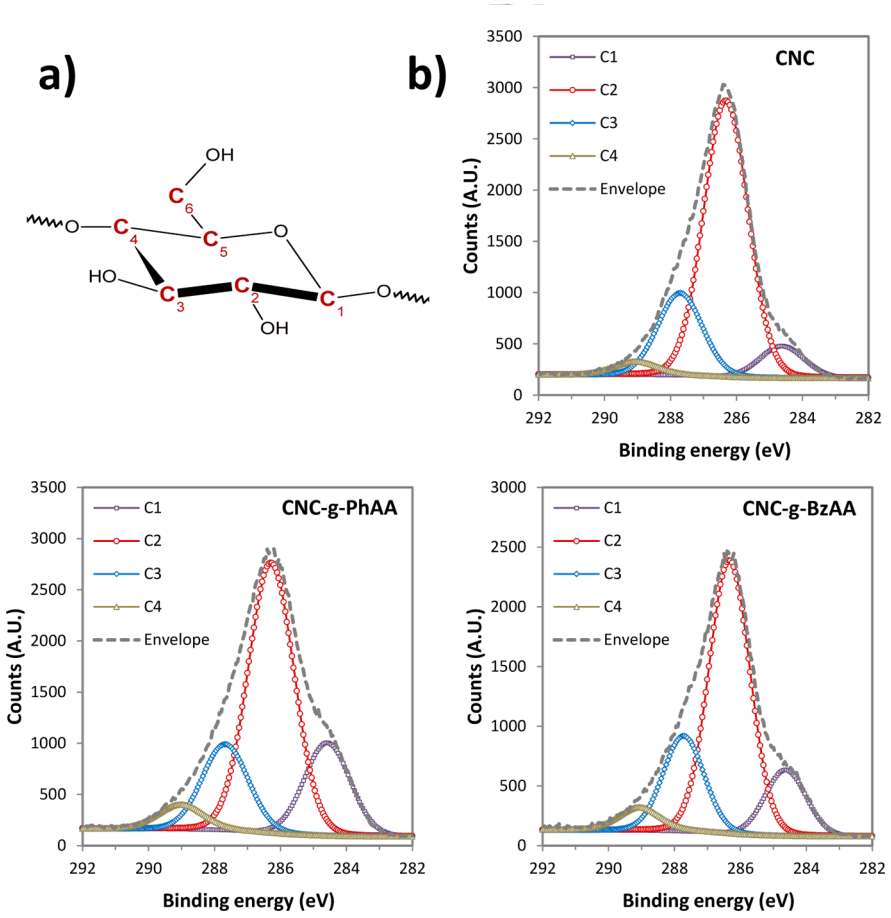

Figure 8. (a) Identification of anhydroglucose unit, and (b) deconvolution of the C 1s peak of neat CNC, CNC-*g*-PhAA, and CNC-*g*-BzAA.

neat CNC can be related to the contamination of glucuronic acid from hemicelluloses. In the present case an increase of the signal was expected because of the ester linkage between the carboxylic acid (PhAA and BzAA) and CNC.

The functionalization with PhAA and BzAA yielded an increase of C1 contribution due to the C−C bonds from the carboxylic acid. More precisely, the signal increased 109.9% after the functionalization with PhAA and 40.13% after functionalization with BzAA. The C4 contribution augmented 38.5% due to the formation of the ester bond with PhAA and 18.6% due to grafting with BzAA. In both cases, the increase was higher for PhAA than BzAA, which showed higher functionalization efficiency using PhAA (deconvoluted molar percent of the different contributions of the C1S peak are founded in Table S3, Supporting Information).

The C1 signal was used for the determination of the degree of surface substitution (DSS), although there is a small error because the C1 contribution is already present in neat CNC due to impurities. The DSS was calculated after

$$\%C1 = \frac{\#\text{of C1 carbons}}{\#\text{of total carbons}} \tag{6}$$

where # of C1 carbons corresponds to the number of C1 carbons of the CA graft per glucose unit, and # of total carbons is the total number of carbon atoms of the grafted glucose unit (AGU + CA). Under these statements the DSS can be integrated in eq 6 by the following formula:

$$\%C1 = \frac{DSS \cdot C_{CA}}{AGU + DSS \cdot CA} \tag{7}$$

where C_{CA} (96.1 and 108.1 g·mol^{-1} for PhAA and BzAA, respectively) and CA (119.1 and 133.2 g·mol^{-1} for PhAA and BzAA, respectively) are the carbon mass and total mass of the grafted carboxylic acid. AGU is the total mass of an anhydroglucose unit (161.1 g·mol^{-1}). Since only one variable is presented in eq 7, the DSS can be calculated from eq 8:

$$DSS = \frac{\%C1 \cdot AGU}{C_{CA} + \%C1 \cdot CA} \tag{8}$$

The DSS of CNC-*g*-PhAA is higher than the one of CNC-*g*-BzAA in concordance with the DS obtained from elemental analysis (Supporting Information, Table S3). We suppose that the grafting of BzAA induced higher steric hindrance or masking of the CNC surface, which brought about lower grafting density. This result evidence that the functionalization took place mainly on the CNC surface. Comparison of DS and DSS shows clearly higher values of surface grafting with values obtained from XPS. This tendency is obvious since the elemental analysis takes into account all the bulk CNC, and not only the surface.

Properties of Functionalized CNC. Thermal degradation of CNC during plastics processing is one challenge for successfully using them in polymer materials. This was studied by thermogravimetric analysis (TGA) and the thermal degradation of pure and modified CNC. Results are plotted in Figure 9. In the case of neat CNC, two principal weight losses were observed at 246 and 303 °C. They are related to the

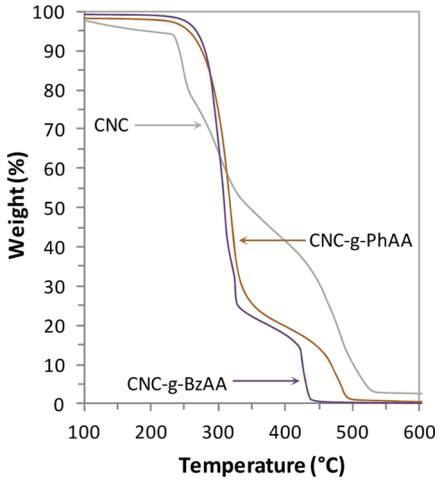

Figure 9. TGA thermograms of pure CNC and modified CNC with PhAA and BzAA.

degradation of CNC−SO_4^{2-} and CNC−OH, respectively, showing that there were still a considerable number of sulfate groups on the CNC surface. The functionalization of CNC yields an improvement in thermal stability of about 10 °C with a single weight loss step below 450 °C. This might be due to the lower amount of surface sulfate groups after grafting as recently detailed.[53] This hypothesis is confirmed by the XPS analysis, which shows the loss of the signal of S 2p after the *SolReact* treatment. It is worth noting the degradation of functionalized CNC was not promoted, as would have been expected if residual acid from the grafting procedure was present. This points to the efficiency of the used washing procedure. In conclusion, the carboxylic acid functionalization did not affect the CNC thermal stability.

One of the main targets of CNC surface modification is to enhance compatibility between the CNC and hydrophobic polymer matrices for their application either as nanoreinforcement or as functional additive in hydrophobic polymer matrices. Therefore, contact angle measurements were carried out to investigate the macroscopic hydrophobicity of functionalized CNC surface. The dried suspensions of CNC resulted with a transparent film. On the contrary, a white powder was obtained upon drying of the grafted CNC. This already confirmed that less hydrogen bonds can be established after surface modification. The dynamic contact angle with a drop of water can be observed in Figure 10, evidencing the more hydrophobic surfaces of grafted CNC. The water contact angle and Young's equation (eq 5) were used to determine the

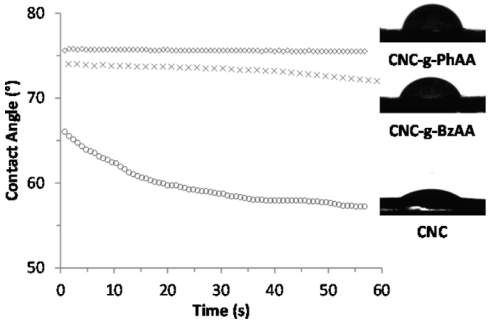

Figure 10. Contact angle measurements of neat CNC (○) and functionalized with PhAA (◇) and BzAA (×).

energy of adhesion (W_{sl}; Table S4 in Supporting Information). The high W_{sl} of neat CNC is caused by highly localized intermolecular forces between the hydroxyl groups of CNC and the water. The breaking of these interactions yields, therefore, a net decrease in W_{sl}. No significant differences of macroscopic surface properties between grafted moieties were observed, though.

The water vapor adsorption isotherm on the unmodified and modified CNC surface was studied by DVS analysis in order to quantify the water vapor adsorption of CNC. The differences related to the nature of the CNC were recorded at two RH, 40% and 80%. The results are shown in Figure 11. At 40% RH

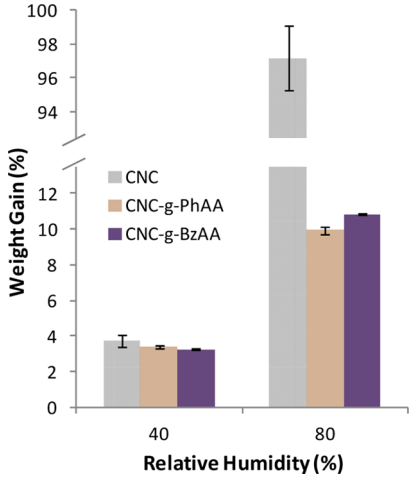

Figure 11. Water vapor adsorption of modified and unmodified CNC placed at 40 and 80% of RH.

there are no significant differences between the neat CNC and the grafted ones. The mass uptake of all samples was around 3.4%. However, once the samples are conditioned in 80% of RH, the unmodified CNC showed almost 100% mass gain, compared to 9.9 and 10.8% for PhAA and BzAA. At low RH, there was no difference between the different types of CNC, probably because water in the gaseous phase can be absorbed on the hydrophilic CNC surface in spite of the presence of the aromatic moieties. At high RH, on the contrary, water apparently condensed on the CNC surface, giving rise to a very high weight uptake. Condension apparently depressed the hydrophobic surface grafts. The surface grafting might therefore also diminish the effects of interaction of CNC nanocomposites with water, such as swelling or higher water permeability, which is often observed upon addition of hydrophilic structures inside apolar polymers.

Recycling of Carboxylic Acids. The *SolReact* procedure uses the reactant as solvent. Therefore, it is interesting to recycle the reactant after the reaction in the aim to decrease the environmental footprint of the reaction, but also to enhance economic feasibility. Therefore, the PhAA and BzAA chemical changes were evaluated by infrared spectroscopy in order to determine a possible change in the functional group vibrations due to the temperature and acid reaction conditions. Figure 12 shows the FT-IR spectra before and after the functionalization of PhAA and BzAA. Clearly, no change in the spectra was observed, which would hint thermal degradation or pollution of the carboxylic acids. Stretching of the carboxyl groups (C═O) is revealed by the band at 1693 cm^{-1}. Signals around 1400−1450 cm^{-1} are related to C−O−H in-plane bend vibrations.

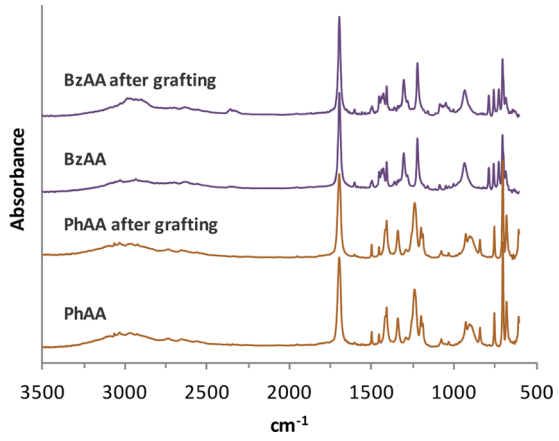

Figure 12. FT-IR spectrum of PhAA and BzAA before and after the grafting reaction.

The C−H group (δ bending) band was found in between 1220 and 1350 cm^{-1}. From the environmental point of view, this kind of functionalization is very promising since the grafting agent can be recycled and reused in subsequent reactions. However, in order to study in detail the purity of the recycled carboxylic acid, sensitive analysis can be done as ^{1}H or ^{13}C NMR.

CONCLUSIONS

A one-pot methodology called *SolReact* was developed for the grafting of nontoxic molecules on the CNC surface. The key point is the use of an in situ solvent exchange strategy for utilizing the grafting reactant as solvent without drying the CNC. The reactant can furthermore be easily recycled and does not suffer from chemical degradation due to moderate reaction temperatures. Surface functionalization was successful and yielded change in macroscopic hydrophobicity of CNC without damaging the crystalline core structure.

The technical simplicity of this one-pot reaction strategy holds the possibility for application in high volume processes or even online in polymer processing.

ASSOCIATED CONTENT

Supporting Information

Physical chemical and safety features of the aromatic carboxylic acids. Experimental and corrected elemental weight composition of neat and modified CNC obtained by elemental analysis and calculated degree of substitution (DS). Elemental mol percent obtained from the O 1s and C 1s peak heights and surface functional group composition obtained from the deconvolution of the peak C 1s from the XPS analysis for modified and unmodified CNC and degree of surface substitution (DSS). Contact angle (deg) and work of adhesion (*Wsl*) of unmodified and modified CNC. This material is available free of charge via the Internet at http://pubs.acs.org.

AUTHOR INFORMATION

Corresponding Author

*E-mail: julien.bras@pagora.grenoble-inp.fr. Tel.: +33 (0)4 76 82 69 15.

Notes

The authors declare no competing financial interest.

ACKNOWLEDGMENTS

The authors wish to express their gratitude to Cecile Sillard for AFM pictures. This work is supported by the Mexican Scholarship Council (CONACyT) under Grant No. 213840. LGP2 is part of the LabEx Tec 21 (Investissements d'Avenir, Grant Agreement No. ANR-11-LABX-0030) and of the Énergies du Futur and PolyNat Carnot Institutes (Investissements d'Avenir, Grant Agreement Nos. ANR-11-CARN-007-01 and ANR-11-CARN-030-01). This work was made possible by the use of specific equipment of the TekLiCell platform supported by Region Rhône-Alpes through FEDER (European fund for regional development) funding.

REFERENCES

(1) Habibi, Y.; Lucia, L. A.; Rojas, O. J. *Chem. Rev.* **2010**, *110*, 3479.
(2) Beecher, J. F. *Nat. Nanotechnol.* **2007**, *2*, 466.
(3) Klemm, D.; Kramer, F.; Moritz, S.; Lindstrom, T.; Ankerfors, M.; Gray, D.; Dorris, A. *Angew. Chem., Int. Ed.* **2011**, *50*, 5438.
(4) Moon, R. J.; Martini, A.; Nairn, J.; Simonsen, J.; Youngblood, J. *Chem. Soc. Rev.* **2011**, *40*, 3941.
(5) Eichhorn, S. J.; Dufresne, A.; Aranguren, M.; Marcovich, N. E.; Capadona, J. R.; Rowan, S. J.; Weder, C.; Thielemans, W.; Roman, M.; Renneckar, S.; Gindl, W.; Veigel, S.; Keckes, J.; Yano, H.; Abe, K.; Nogi, M.; Nakagaito, A. N.; Mangalam, A.; Simonsen, J.; Benight, A. S.; Bismarck, A.; Berglund, L. A.; Peijs, T. *J. Mater. Sci.* **2010**, *45*, 1.
(6) Rånby, B. G. *Acta Chem. Scand.* **1949**, *3*, 649.
(7) Rånby, B. G. *Discuss. Faraday Soc.* **1951**, *11*, 164.
(8) Rånby, B. G. *Experientie* **1950**, *6*, 12.
(9) Bondeson, D.; Mathew, A.; Oksman, K. *Cellulose* **2006**, *13*, 171.
(10) Dong, X. M.; Revol, J. F.; Gray, D. G. *Cellulose* **1998**, *5*, 19.
(11) Beck-Candanedo, S.; Roman, M.; Gray, D. G. *Biomacromolecules* **2005**, *6*, 1048.
(12) Siqueira, G.; Bras, J.; Dufresne, A. *Polymers* **2010**, *2*, 728.
(13) Dufresne, A. *Nanocellulose: From Nature to High Performance Tailored Materials*; Walter de Gruyter and Co.: Berlin, 2012.
(14) Charreau, H.; Foresti, M. L.; Vazquez, A. *Recent Pat. Nanotechnol.* **2013**; Vol. 7, p 25.
(15) Lin, N.; Huang, J.; Dufresne, A. *Nanoscale* **2012**, *4*, 3274.
(16) Mariano, M.; El Kissi, N.; Dufresne, A. *J. Polym. Sci., Part B: Polym. Phys.* **2014**, *52*, 791.
(17) Chauve, G.; Bras, J. In *Handbook of Green Materials: Processing Technologies, Properties and Applications*; Oksman, K., Bismarck, A., Rojas, O., Sain, M., Eds.; World Scientific: River Edge, NJ, 2014; Vol. *1*.
(18) Habibi, Y. *Chem. Soc. Rev.* **2014**, *43*, 1519.
(19) Fortunati, E.; Peltzer, M.; Armentano, I.; Torre, L.; Jimenez, A.; Kenny, J. M. *Carbohydr. Polym.* **2012**, *90*, 948.
(20) Hasani, M.; Cranston, E. D.; Westman, G.; Gray, D. G. *Soft Matter* **2008**, *4*, 2238.
(21) Salajkova, M.; Berglund, L. A.; Zhou, Q. *J. Mater. Chem.* **2012**, *22*, 19798.
(22) Gousse, C.; Chanzy, H.; Excoffier, G.; Soubeyrand, L.; Fleury, E. *Polymer* **2002**, *43*, 2645.
(23) Berlioz, S.; Molina-Boisseau, S.; Nishiyama, Y.; Heux, L. *Biomacromolecules* **2009**, *10*, 2144.
(24) Shang, W. L.; Huang, J.; Luo, H.; Chang, P. R.; Feng, J. W.; Xie, G. Y. *Cellulose* **2013**, *20*, 3247.
(25) de Menezes, A. J.; Siqueira, G.; Curvelo, A. A. S.; Dufresne, A. *Polymer* **2009**, *50*, 4552.
(26) Taipina, M. D.; Ferrarezi, M. M. F.; Yoshida, I. V. P.; Goncalves, M. D. *Cellulose* **2013**, *20*, 217.
(27) Siqueira, G.; Bras, J.; Dufresne, A. *Langmuir* **2010**, *26*, 402.
(28) Rueda, L.; d'Arlas, B. F.; Zhou, Q.; Berglund, L. A.; Corcuera, M. A.; Mondragon, I.; Eceiza, A. *Compos. Sci. Technol.* **2011**, *71*, 1953.
(29) Yuan, H. H.; Nishiyama, Y.; Wada, M.; Kuga, S. *Biomacromolecules* **2006**, *7*, 696.

(30) Kan, K. H. M.; Li, J.; Wijesekera, K.; Cranston, E. D. *Biomacromolecules* **2013**, *14*, 3130.
(31) Tehrani, A. D.; Neysi, E. *Carbohydr. Polym.* **2013**, *97*, 98.
(32) Morandi, G.; Heath, L.; Thielemans, W. *Langmuir* **2009**, *25*, 8280.
(33) Espino, E.; Bras, J.; Gilbert, R.; Belgacem, N.; Domenek, S.; Dufresne, A. In 245th ACS National Meeting − Division of Cellulose and Renewable Materials, New Orleans, Louisiana, USA, April 7−11, 2013, American Chemical Society: Washington, DC, 2013.
(34) Goffin, A.-L.; Raquez, J.-M.; Duquesne, E.; Siqueira, G.; Habibi, Y.; Dufresne, A.; Dubois, P. *Biomacromolecules* **2011**, *12*, 2456.
(35) Labet, M.; Thielemans, W. *Cellulose* **2011**, *18*, 607.
(36) Anastas, P.; Eghbali, N. *Chem. Soc. Rev.* **2010**, *39*, 301.
(37) Filpponen, I.; Argyropoulos, D. S. *Biomacromolecules* **2010**, *11*, 1060.
(38) Akhlaghi, S. P.; Tam, K. C.; Beery, R. In *Patentscope* 2014.
(39) Kloser, E.; Gray, D. G. *Langmuir* **2010**, *26*, 13450.
(40) Zhang, J.; Kwok, D. Y. *J. Phys. Chem. B* **2002**, *106*, 12594.
(41) Marchessault, R. H.; Morehead, F. F.; Walter, N. M. *Nature* **1959**, *184*, 632.
(42) Filson, P. B.; Dawson-Andoh, B. E.; Schwegler-Berry, D. *Green Chem.* **2009**, *11*, 1808.
(43) Sèbe, G.; Ham-Pichavant, F.; Pecastaings, G. *Biomacromolecules* **2013**, *14*, 2937.
(44) Cartier, N.; Escaffre, P.; Mathevet, F.; Chanzy, H.; Vuong, R. *Tappi J.* **1994**, *77*, 95.
(45) Sèbe, G.; Ham-Pichavant, F.; Ibarboure, E.; Koffi, A. L. C.; Tingaut, P. *Biomacromolecules* **2012**, *13*, 570.
(46) Park, S.; Baker, J.; Himmel, M.; Parilla, P.; Johnson, D. *Biotechnol. Biofuels* **2010**, *3*, 1.
(47) Ioelovich, M. *ISRN Chem. Eng,* **2012**, *2012*, 7.
(48) Maddahy, N. K.; Ramezani, O.; Kermanian, H. In 4th International Conference on Nanostructures (ICNS4), Kish Island, Iran, March 12−14, 2012, Sharif University of Technology: Tehran, Iran, 2012.
(49) Rosa, M. F.; Medeiros, E. S.; Malmonge, J. A.; Gregorski, K. S.; Wood, D. F.; Mattoso, L. H. C.; Glenn, G.; Orts, W. J.; Imam, S. H. *Carbohydr. Polym.* **2010**, *81*, 83.
(50) Belgacem, M. N.; Czeremuszkin, G.; Sapieha, S.; Gandini, A. *Cellulose* **1995**, *2*, 145.
(51) Gu, J.; Catchmark, J. M.; Kaiser, E. Q.; Archibald, D. D. *Carbohydr. Polym.* **2013**, *92*, 1809.
(52) Dufresne, A.; De Gruyter: Berlin, 2012.
(53) Beck, S.; Bouchard, J. *Nord. Pulp Pap. Res. J.* **2014**, *29*, 8.